Geometries, Bonding Nature, and Relative Stabilities of Dinuclear Palladium(I) π-Allyl and Mononuclear Palladium(II) π-Allyl Complexes. A Theoretical Study

Shigeyoshi Sakaki,* Kaori Takeuchi, and Manabu Sugimoto

Department of Applied Chemistry and Biochemistry, Faculty of Engineering, Kumamoto University, Kurokami, Kumamoto 860, Japan

Hideo Kurosawa

Department of Applied Chemistry, Faculty of Engineering, Osaka University, Suita, Osaka 565, Japan

Received February 14, 1997[⊗]

MP2 optimization of $Pd_2(\mu\text{-Br})(\mu\text{-}C_3H_5)(PH_3)_2$ (**1**) and $PdCl(\eta^3\text{-}C_3H_5)(PH_3)$ (**2**) well reproduces geometrical characteristics of these complexes. For instance, the optimized dihedral angle between π-allyl and Pd_2Br planes is 83° in **1**, and the dihedral angle between π-allyl and $PdCl(PH_3)$ planes is 115° in **2**. These optimized values agree well with the experimental results (the deviation is less than 1°). Although the π-allyl coordinate bond of **2** is mainly formed by donation from the π-allyl nonbonding π (nπ) orbital to the unoccupied d orbital of Pd, the μ-allyl coordinate bond of **1** is formed by back-donation from the Pd−Pd d_σ bonding orbital to the π-allyl π^* orbital and donation from the π-allyl nπ orbital to the Pd−Pd d_σ antibonding orbital. To maximize these two interactions, two palladium atoms take their positions under the terminal carbon atoms of μ-allyl group. In addition to these interactions, the back-donating interaction between the μ-allyl π^* and the Pd−Pd d_π bonding orbitals participates in the μ-allyl coordination. The dihedral angle θ of **1** decreases to 83° to enhance the above-mentioned two back-bonding interactions. Introduction of the electron-withdrawing CN group to π-allyl enhances the stability of **1** and decreases the dihedral angle θ. However, introduction of the electron-releasing CH_3 group to π-allyl little changes the dihedral angle of **1** but enhances the stability of **2**. These substituent effects, as well as the difference in the dihedral angle between **1** and **2**, are clearly interpreted in terms of the coordinate bonding nature.

Introduction

Multinuclear organotransition metal complexes are a particularly attractive subject of research, since their coordinate bond is considered as a good model of surface−hydrocarbon interaction.[1] In this regard, detailed theoretical investigation is necessary to understand well the multiple site interaction of an organic molecule with a multinuclear metal complex. A dinuclear palladium(I) μ-allyl complex, $Pd_2(\mu\text{-X})(\mu\text{-}C_3H_5)(PH_3)_2$,[2−9] seems to be a prototypical multinuclear organotransition metal complex, and it is suitable for detailed theoretical investigation because of its relatively small size and symmetrical structure. This complex exhibits several characteristic geometrical features:[3,5e,7,8b] (1) two palladium atoms take their positions under the terminal carbon (C_t) atoms of the μ-allyl ligand; (2) the Pd−Pd distance is about 2.6 Å, indicating the presence of a Pd−Pd bond; and (3) the dihedral angle between π-allyl and Pd_2X planes is about 85° (smaller than 90°) which is in clear contrast to the large dihedral angle of 110−125° in mononuclear palladium(II) π-allyl complexes.[9] These geometrical features are deeply related to the bonding nature and the electron distribution. In spite of these interesting

[⊗] Abstract published in *Advance ACS Abstracts,* June 1, 1997.

(1) (a) Holton, J.; Lappert, M. F.; Pearce, R.; Yarrow, P. I. W. *Chem. Rev.* **1983**, *83*, 135. (b) Stone, F. G. A. *Angew. Chem., Int. Ed. Engl.* **1984**, *23*, 89. (c) Casey, C. P.; Audett, J. D. *Chem. Rev.* **1986**, *86*, 339. (d) Wadepohl, H. *Angew. Chem., Int. Ed. Engl.* **1992**, *31*, 247. (e) Beck, W.; Niemer, B.; Wieser, M. *Angew. Chem., Int. Ed. Engl.* **1993**, *32*, 923 and references therein.

(2) Werner, H. *Adv. Organomet. Chem.* **1981**, *19*, 155. Maillis, P. M.; Russell, M. J. H. In *Comprehensive Organometallic Chemistry*; Wilkinson, G., Ed.; Pergamon: Oxford, 1982; Vol. 6, p 265 and references therein.

(3) Kobayashi, Y.; Iitaka, Y.; Yamazaki, H. *Acta Crystallogr.* **1972**, *B28*, 889.

(4) (a) Werner, H.; Tune, D.; Parker, G.; Krüger, C.; Brauer, D. J. *Angew. Chem., Int. Ed. Engl.* **1975**, *14*, 185. (b) Werner, H.; Kühn, A. *Angew. Chem., Int. Ed. Engl.* **1977**, *16*, 412. (c) Werner, H.; Kühn, A.; Tune, D. J.; Krüger, C.; Braner, D. J.; Sekutowski, J. C.; Tsay, Y.-H. *Chem. Ber.* **1977**, *110*, 1763. (d) Werner, H.; Kühn, A. *Angew. Chem., Int. Ed. Engl.* **1979**, *18*, 416. (e) Kühn, A.; Werner, H. *J. Organomet. Chem.* **1979**, *179*, 421. (f) Werner, H.; Kraus, H. J. *Chem. Ber.* **1980**, *113*, 1072.

(5) (a) Yamamoto, T.; Saito, O.; Yamamoto, A. *J. Am. Chem. Soc.* **1981**, *103*, 5600. (b) Yamamoto, T.; Akimoto, M.; Saito, O.; Yamamoto, A. *Organometallics* **1986**, *5*, 1559. (c) Osakada, K.; Chiba, T.; Nakamura, Y.; Yamamoto, T.; Yamamoto, A. *J. Chem. Soc., Chem. Commun.* **1986**, 1589. (d) Osakada, K.; Chiba, T.; Nakamura, Y.; Yamamoto, T.; Yamamoto, A. *Organometallics* **1989**, *8*, 2602. (e) Osakada, K.; Ozawa, Y.; Yamamoto, A. *J. Organomet. Chem.* **1990**, *399*, 341.

(6) Hayashi, Y.; Matsumoto, K.; Nakamura, Y.; Isobe, K. *J. Chem. Soc., Dalton. Trans.* **1989**, 1519.

(7) Sieler, J.; Helms, M.; Gaube, W.; Svensson, A.; Lindquist. O. *J. Organomet. Chem.* **1987**, *320*, 129.

(8) (a) Miyauchi, Y.; Watanabe, S.; Kuniyasu, H.; Kurosawa, K. *Organometallics* **1995**, *14*, 5450. (b) Kurosawa, H.; Hirako, K.; Natsume, S.; Ogoshi, S.; Kanehisa, N.; Kai, Y.; Sakaki, S.; Takeuchi, K. *Organometallics* **1996**, *15*, 2089.

(9) (a) Maitlis, P. M.; Espinet, P.; Russell, M. J. H. in *Comprehensive Organometallic Chemistry*; Wilkinson, G., Ed.; Pergamon: Oxford, 1982; Vol. 6, p 385. (b) Hartley, F. R. *The Chemistry of Platinum and Palladium*; Applied Science Publ.: London, 1973; p 430 and references therein.

S0276-7333(97)00115-5 CCC: $14.00

Chart 1

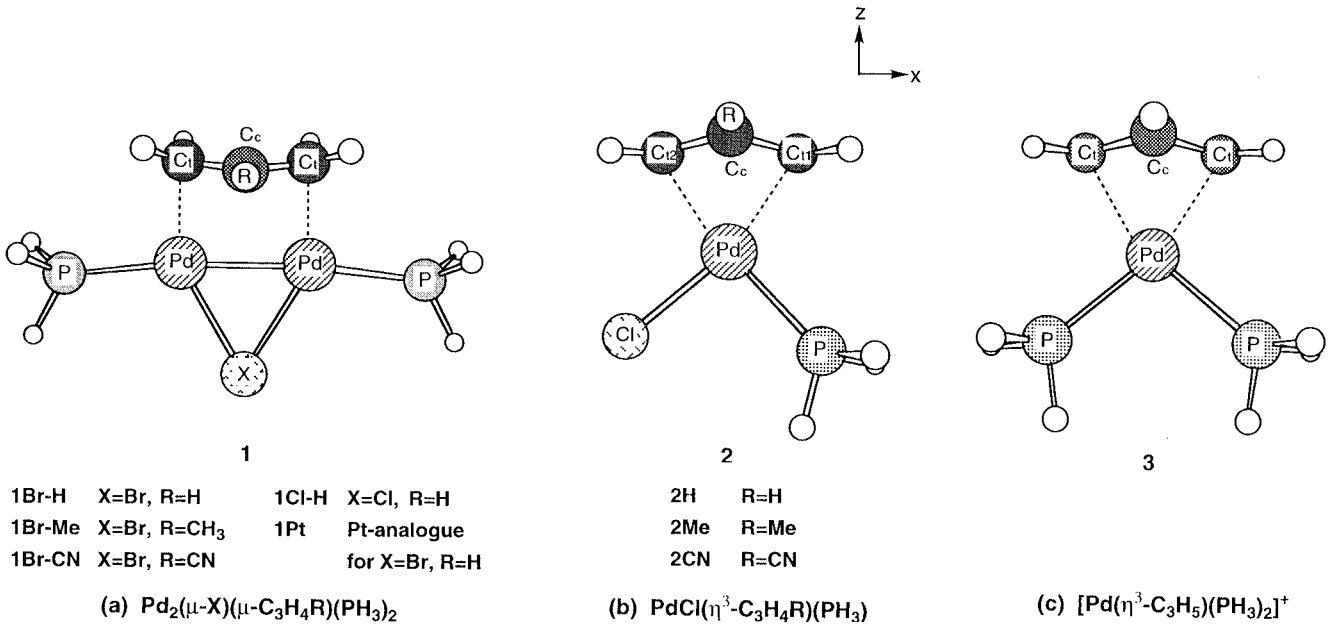

1Br-H	X=Br, R=H	1Cl-H	X=Cl, R=H
1Br-Me	X=Br, R=CH_3	1Pt	Pt-analogue
1Br-CN	X=Br, R=CN		for X=Br, R=H

2H	R=H
2Me	R=Me
2CN	R=CN

(a) $Pd_2(\mu\text{-}X)(\mu\text{-}C_3H_4R)(PH_3)_2$ (b) $PdCl(\eta^3\text{-}C_3H_4R)(PH_3)$ (c) $[Pd(\eta^3\text{-}C_3H_5)(PH_3)_2]^+$

issues, geometries, electron distribution, and bonding nature of multinuclear μ-allyl complexes have been only qualitatively discussed on the basis of an orbital interaction diagram so far,[10−12] and a detailed theoretical investigation of their geometries and bonding nature has not been carried out yet, to our knowledge.

In this theoretical work, we performed ab initio MO/MP2-MP4 calculations of dinuclear palladium(I) μ-allyl complexes, $Pd_2(\mu\text{-Br})(\mu\text{-}CH_2CRCH_2)(PH_3)_2$ (**1Br-R**, R = H, CH_3, or CN), $Pd_2(\mu\text{-Cl})(\mu\text{-}C_3H_5)(PH_3)_2$ (**1Cl-H**), and $Pt_2(\mu\text{-Br})(\mu\text{-}C_3H_5)(PH_3)_2$ (**1Pt**), and mononuclear palladium(II) π-allyl complexes, $PdCl(\eta^3\text{-}CH_2CRCH_2)(PH_3)$ (**2R**) and $[Pd(\eta^3\text{-}C_3H_5)(PH_3)_2]^+$ (**3**) (see Chart 1). Our purposes here are (1) to present a theoretical understanding of the μ-allyl coordinate bond of **1**, (2) to clarify the differences in the π-allyl coordinate bond between dinuclear palladium(I) μ-allyl and mononuclear palladium(II) π-allyl complexes, and (3) to elucidate the reason that the dihedral angle between π-allyl and a molecular plane is smaller than 90° in **1** but larger than 90° in **2** and **3**, since these geometrical features have been discussed as important characteristic differences between dinuclear palladium(I) and mononuclear palladium(II) π-allyl complexes and no conclusive explanation seems to have been given yet.[8b,10]

Computational Details

Geometries of all the complexes were optimized at the MP2 level, where the C_s symmetry was adopted and the geometry of PH_3 was taken to be the same as that of the free PH_3 molecule.[13] Then, MP2-MP4SDQ calculations were carried out on those optimized geometries. Gaussian 92[14a] and 94[14b] programs were used for these calculations.

Two kinds of basis set systems were used. In both, core electrons of Pd (up to 3d), Pt (up to 4f),[15] P (up to 2p), Cl (up to 2p), and Br (up to 3d)[16] were replaced with effective core potentials (ECPs). In the smaller basis set system (BS-I), valence electrons of Pd and Pt were represented with (5s 5p 4d)/[3s 3p 2d] and (5s 5p 3d)/[3s 3p 2d] sets, respectively,[15] and those of P, Cl, and Br were represented with (3s 3p)/[2s 2p] sets.[16] We adopted here the double-ζ contraction for d electrons of Pd and Pt, since both double-ζ and triple-ζ contractions yield almost the same optimized geometries.[8b] For C and H atoms, MIDI-3[17] and (4s)/[2s][18] sets were used, respectively, where a d-polarization function (ζ = 0.60) was added to the C atom. The importance of a d-polarization function on C will be discussed below. This BS-I system was used for the geometry optimization. In the larger basis set system (BS-II), the ECPs used for Pd, Pt, P, Cl, and Br were taken to be the same as those in the BS-I, but slightly more flexible (5s 5p 4d)/[3s 3p 3d] and (5s 5p 3d)/[3s 3p 3d] basis sets were used for valence electrons of Pd and Pt, respectively. The Huzinaga-Dunning (9s 5p)/[3s 2p] basis set was used for all the first-row elements with a d-polarization function (ζ = 0.75 for C and 0.80 for N),[18] while the basis sets for H, Cl, Br, and P atoms were taken to be the same as those in the BS-I.

Results and Discussion

Basis Set and Electron Correlation Effects on Optimized Geometries. First, we tried to optimize the geometry of $Pd_2(\mu\text{-Br})(\mu\text{-}C_3H_5)(PH_3)_2$ (**1Br-H**, see Chart 1) at the SCF level using the BS-I set with a d-polarization function excluded from the C atom.

(10) Chisholm, M. H.; Hampden-Smith, M. J.; Huffman, J. C. *J. Am. Chem. Soc.* **1988**, *110*, 4070.
(11) Zhu, L.; Kostić, N. M. *Organometallics* **1988**, *7*, 665.
(12) Housecroft, C. E.; Johnson, B. F. G.; Lewis, J.; Lunniss, J. A.; Owen, S. M.; Raithby, P. R. *J. Organomet. Chem.* **1991**, *409*, 271.
(13) Herzberg, G. *Molecular Spectra and Molecular Structure*; D. Van Nostrand Co. Inc.: Princeton, NJ, 1967; Vol. 3, p 610.
(14) (a) Frisch, M. J.; Trucks, G. W.; Head-Gordon, M.; Gill, P. M. W.; Wong, M. W.; Foresman, J. B.; Johnson, B. G.; Schlegel, H. B.; Robb, M. A.; Replogle, E. S.; Gomperts, R.; Andres, J. L.; Raghavachari, K.; Binkley, J. S.; Gonzalez, C.; Martin, R. L.; Fox, D. J.; DeFrees, D. J.; Baker, J.; Stewart, J. J. P.; Pople, J. A. *Gaussian 92*; Gaussian Inc.: Pittsburgh, PA, 1992. (b) Frisch, M. J.; Trucks, G. W.; Schlegel, H. B.; Gill, P. M. W.; Johnson, B. G.; Robb, M. A.; Cheeseman, J. R.; Keith, T. A.; Petersson, G. A.; Montgomery, J. A.; Raghavachari, K.; Al-Laham, M. A.; Zakrzewski, V. G.; Ortiz, J. V.; Foresman, J. B.; Cioslowski, J.; Stefanov, B. B.; Nanayakkara, A.; Challacombe, M.; Peng, C. Y.; Ayala, P. Y.; Chen, W.; Wong, M. W.; Andres, J. L.; Replogle, E. S.; Gomperts, R.; Martin, R. L.; Fox, D. J.; Binkley, J. S.; Defrees, D. J.; Baker, J.; Stewart, J. P.; Head-Gordon, M.; Gonzalez, C.; Pople, J. A. *Gaussian 94*; Gaussian, Inc.: Pittsburgh, PA, 1995.
(15) Hay, P. J.; Wadt, W. R. *J. Chem. Phys.* **1985**, *82*, 299.
(16) Wadt, W. R.; Hay, P. J. *J. Chem. Phys.* **1985**, *82*, 284.
(17) Huzinaga, S.; Andzelm, J.; Klobkowski, M.; Radio-Andzelm, E.; Sakai, Y.; Tatewaki, H. *Gaussian Basis Sets for Molecular Calculations*; Elsevier: Amsterdam, 1984.
(18) Dunning, T. H.; Hay, P. J. In *Methods of Electronic Structure Theory*; Schaefer, H. F., Ed.; Plenum: New York, 1977; p 1.

Table 1. Optimized Geometrical Parameters of $Pd_2(\mu\text{-}X)(\mu\text{-}C_3H_5)(PH_3)_2$

	$Pd_2(\mu\text{-Br})(\mu\text{-}C_3H_5)(PH_3)_2$					$Pd_2(\mu\text{-Cl})(\mu\text{-}C_3H_5)(PH_3)_2$		
	HF		MP2			MP2		
	no d[a]	with d[b]	no d[a]	with d[b]	exptl[c]	no d[a]	with d[b]	exptl[d]
M−M	2.613	2.619	2.648	2.635	2.642	2.633	2.621	2.623
$M-C_t$	2.123	2.090	2.177	2.115	2.082	2.172	2.110	2.07
$M-C_c$	2.556	2.518	2.592	2.518	2.470	2.582	2.508	2.455_{av}
M−X	2.718	2.730	2.619	2.624	2.533	2.526	2.530	2.436_{av}
M−P	2.557	2.562	2.404	2.402	2.277	2.404	2.403	2.286_{av}
C_t-C_c	1.411	1.417	1.428	1.427	1.429	1.430	1.429	1.385_{av}
θ[e]	88	87	86	83	83.7	85	83	82.1

[a] Without d-polarization function on the C atom. [b] With d-polarization function on the C atom. [c] $Pd_2(\mu\text{-Br})(\mu\text{-}C_3H_4COOCH_3)_2$; ref 8b. [d] $Pd_2(\mu\text{-Cl})(\mu\text{-}C_3H_5)(PPh_3)_2$; ref 7. [e] The dihedral angle between the μ-allyl and $Pd_2(\mu\text{-X})$ planes.

Table 2. Optimized Geometrical Parameters of $PdCl(\eta^3\text{-}C_3H_5)(PH_3)$ and $Pd(PH_3)(\eta^3\text{-}C_3H_5)$

	$PdCl(\eta^3\text{-}C_3H_5)(PH_3)$					$[Pd(\eta^3\text{-}C_3H_5)(PH_3)_2]^+$	
	HF	MP2		expt		MP2	
	no d[a]	no d[a]	with d[b]	*c*	*d*	with d[b]	exptl[e]
$M-C_{t1}$	2.183	2.267	2.177	2.201	2.14	2.202	2.189
$M-C_{t2}$	2.196	2.226	2.148	2.193	2.28	2.202	2.178
$M-C_c$	2.229	2.236	2.143	2.116	2.22	2.193	2.205
C_c-C_{t1}	1.403	1.418	1.414	1.379	1.47	1.412	1.404
C_c-C_{t2}	1.392	1.422	1.416	1.347	1.40	1.412	1.396
θ[f]	120	115	115	114.5	116	114	120.1[g]

[a] Without d-polarization function on the C atom. [b] With d-polarization function on the C atom. [c] $Pd(SnCl_3)(\eta^3\text{-}C_3H_5)(PPh_3)$; ref 19. [d] $PdCl(\eta^3\text{-}C_4H_7)(PPh_3)$; ref 20. [e] $[Pd(\eta^3\text{-}C_4H_7)(PMe_3)_2]^+$; ref 21. [f] The dihedral angle between the μ-allyl and $PdX(PH_3)$ planes. [g] Estimated using data given in ref 21.

The optimized dihedral angle is much larger than the experimental value, as shown in Table 1. Addition of the d-polarization function to the C atom little improves the dihedral angle at the SCF level but significantly improves it at the MP2 level. The MP2/BS-I-optimized dihedral angle is almost the same as the experimental value. Even at the MP2 level, this dihedral angle was too large if no d-polarization function was added to the C atom. The necessity of a d-polarization function in **1** suggests that the frontier orbitals of μ-allyl should be flexible to overlap well with the d orbital of the $Pd_2(\mu\text{-X})(PH_3)_2$ part. The geometry of $Pd_2(\mu\text{-Cl})(\mu\text{-}C_3H_5)(PH_3)_2$ (**1Cl-H**) was optimized with the MP2/BS-I method. As shown in Table 1, the optimized dihedral angle of this complex also agrees well with the experimental value[7] when the d-polarization function is added to the C atom. Not only the dihedral angle but also the geometry of the $Pd_2(\mu\text{-allyl})$ part, such as C−C and $Pd-C_t$ distances and the CPdP angle (96°; exptl[7] = 96.86°), do not deviate very much from the experimental geometry.

The geometry optimization of **2H** was also carried out at both SCF and MP2 levels, as shown in Table 2. Although the geometry optimization at the SCF level yields a somewhat smaller dihedral angle than the experimental one, the MP2-optimized dihedral angle agrees well with the experimental value even when no d-polarization function is added on the C atom. Considering the importance of the d-polarization function in MP2 optimization of **1**, all the complexes examined here were optimized at the MP2 level with the BS-I set, which was augmented with a d-polarization function added on the C atom.

Here, we need to mention that the calculated Pd−Br, Pd−Cl, and $Pd-PH_3$ bond distances of **1Br-H**, **1Cl-H**, and **2H** are somewhat longer than the experimental values; for **1Br-H** and **1Cl-H**, see Table 1, and for **2H**, Pd−Cl = 2.443 Å (exptl[19,20] = 2.563 and 2.38 Å) and Pd−P = 2.443 Å (exptl[19,20] = 2.317 and 2.31 Å). Our previous investigation[22] clearly indicated that the addition of a d-polarization function on the P atom significantly improves the optimized $Pd-PH_3$ bond distance. However, the addition of d-polarization functions on halogen and P atoms remarkably increases the numbers of basis set functions. Moreover, the geometry of the $Pd_2(\mu\text{-allyl})$ part of **1** was successfully optimized with the MP2/BS-I calculation. Thus, the MP2/BS-I optimization seems reliable enough for investigating the electron distribution and coordinate bond nature of **1** and **2**.

In Figure 1, the total energies of **1Br-H** and **2H** are given as a function of the dihedral angle, where the BS-II was used. Apparently, the MP2 calculation yields almost the same energy minimum as the MP3-MP4 calculations. Although the SCF calculation yields a slightly different dihedral angle than MP2-MP4 calculations, the SCF-optimized angle is smaller than 90° in **1Br-H** and larger than 90° in **2H**. This would support the idea that a Walsh diagram is useful for investigating the reason that the dihedral angle is considerably different between **1Br-H** and **2H**.

Electron Distribution and Orbital Interaction Diagram. First, we will briefly examine the orbital interaction diagram prior to detailed discussion. Frontier orbitals of the π-allyl anion are π, nonbonding π (nπ), and π* orbitals (Chart 2), in which HOMO is nπ and LUMO is π*. Important molecular orbitals of $[Pd_2(\mu\text{-Br})(PH_3)_2]^+$ are also given in Chart 2; since the

(19) (a) Mason, R.; Whimp, P. O. *J. Chem. Soc. (A)* **1969**, 2709. (b) Mason, R.; Robertson, G. B.; Whimp, P. O.; White, D. A. *Chem. Commun.* **1968**, 1655.
(20) Mason, R.; Russell, D. R. *Chem. Commun.* **1966**, 26.
(21) Ozawa, F.; Son, T.; Ebina, S.; Osakada, K.; Yamamoto, A. *Organometallics* **1992**, *11*, 171.
(22) Sakaki, S.; Satoh, H.; Shono, H.; Uzino, Y. *Organometallics* **1996**, *15*, 1713.
(23) In the parentheses of $\psi(\phi^b(d_{x^2-y^2})\text{-}\pi^*)$ etc., the first component contributes more to ψ than the latter component. The superscripts a and b represent antibonding molecular orbital (MO) and bonding MO, respectively.

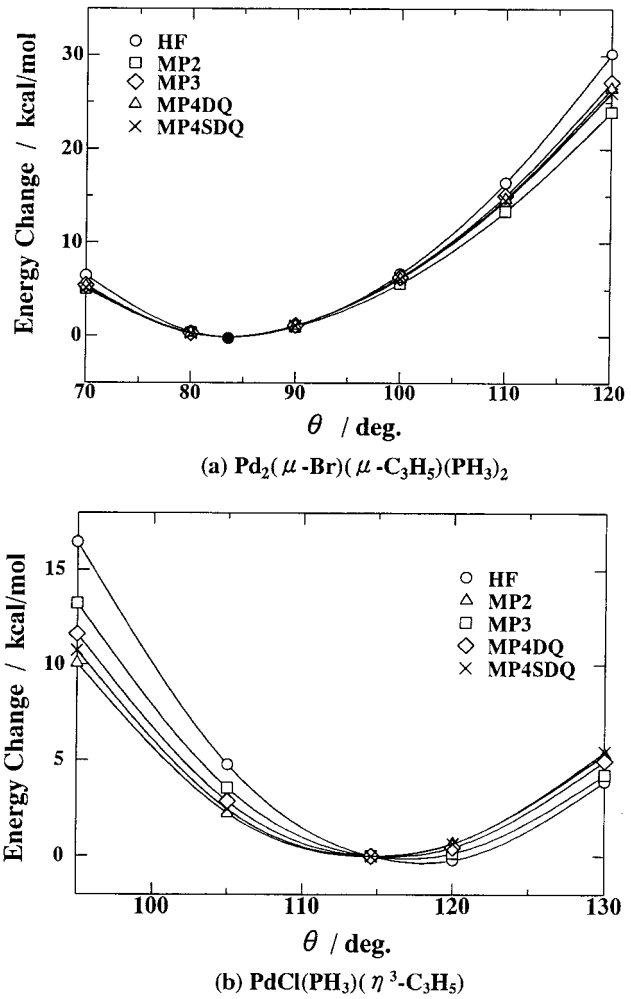

Figure 1. Total energies vs dihedral angle between the π-allyl and molecular planes. (a) The values given here are total energies relative to the MP2-optimized geometry.

palladium(I) atom has a d^9 electron configuration, LUMO is $\phi^a(d_{x^2-z^2})$, involving the antibonding interaction between $d_{x^2-z^2}$ orbitals of two Pd atoms, and HOMO is $\phi^b(d_{x^2-z^2})$, involving the bonding interaction between $d_{x^2-z^2}$ orbitals of two Pd atoms, where superscripts a and b represent antibonding molecular orbital (MO) and bonding MO, respectively. This means that a single covalent bond exists between two palladium(I) atoms. The next HOMO is not the d_{xz}-d_{xz} antibonding orbital $\phi^a(d_{xz})$ but the d_{xz}-d_{xz} bonding orbital $\phi^b(d_{xz})$. Here, we need to mention the reason that $\phi^b(d_{xz})$ is at a higher energy than $\phi^a(d_{xz})$. The $\phi^b(d_{xz})$ involves the antibonding mixing of the Br p orbital, as schematically shown in Chart 3A. On the other hand, the antibonding mixing of the Br p orbital occurs little in $\phi^a(d_{xz})$, probably due to the poor overlap between Br p and Pd d_{xz} orbitals (Chart 3B), whereas such overlap is possible from the symmetry. Thus, $\phi^b(d_{xz})$ is at a higher energy than $\phi^a(d_{xz})$.

The π-allyl nπ orbital overlaps well with $\phi^a(d_{x^2-z^2})$ to form the donating interaction in which charge transfer (CT) occurs from the π-allyl anion to $[Pd_2(\mu\text{-X})(PH_3)_2]^+$. The π-allyl π^* orbital overlaps well with $\phi^b(d_{x^2-z^2})$ to form the back-donating interaction in which CT occurs from $[Pd_2(\mu\text{-X})(PH_3)_2]^+$ to the π-allyl anion. Two Pd atoms take their positions under the terminal carbon (C_t) atoms of μ-allyl, so as to maximize the overlap between π-allyl nπ and $\phi^a(d_{x^2-z^2})$ orbitals and the overlap between π-allyl π^* and $\phi^b(d_{x^2-z^2})$ orbitals. At the same time, $\phi^b(d_{xz})$ can overlap with the π-allyl π^* orbital. If the dihedral angle decreases to 85° from 90°, the p_π orbital of the π-allyl central carbon (C_c) atom becomes favorable for the overlap with $\phi^b(d_{x^2-z^2})$ and $\phi^b(d_{xz})$, which strengthens the back-donating interaction to the π-allyl anion from $[Pd_2(\mu\text{-Br})(PH_3)_2]^+$ (Chart 4).

A possible orbital interaction diagram for **2** is also shown in Chart 2B. The d_{xz} orbital is LUMO of $[PdCl(PH_3)]^+$ and interacts with the π-allyl nπ orbital to form the donating interaction from the π-allyl anion to Pd(II). The π-allyl π orbital suffers from an antibonding mixing of the $d_{x^2-z^2}$ orbital, since the $d_{x^2-z^2}$ orbital is at a lower energy than the π orbital. The Pd s and p_z orbitals might also overlap with the π-allyl π orbital in a bonding way to weaken the above-described antibonding overlap. The Pd d_{yz} orbital might overlap with the π-allyl π^* orbital to form the back-donating interaction from Pd(II) to the π-allyl anion if the d_{yz} orbital is at a high energy.

Considering the above-mentioned possible interactions, we will start to discuss the electron distribution and coordinate bonding nature. Interestingly, the Pd atomic charge is similar in **1** and **2**, as shown in Table 3, where natural bond orbital (NBO) populations[24] are given. However, the charge of the π-allyl part is significantly different between dinuclear Pd(I) μ-allyl complexes (**1**) and mononuclear Pd(II) π-allyl complexes (**2** and **3**); the π-allyl part is negatively charged in **1** but positively charged in **2** and **3**. This difference clearly indicates that the donating interaction is stronger in **2** and **3** than in **1** and/or the back-donating interaction is stronger in **1** than in **2** and **3**.

Why Does 1 Have the Small Dihedral Angle (θ) between π-Allyl and Pd_2Br Planes, and Why Do 2 and 3 Have the Large Dihedral Angle (θ)? A Walsh diagram of $Pd_2(\mu\text{-Br})(\mu\text{-}C_3H_5)(PH_3)_2$ (**1Br-H**) provides us clear pictures of the bonding nature. As shown in Figure 2, $\psi(\phi^b(d_{x^2-z^2})\text{-}\pi^*)$,[23] which involves the bonding interaction between π-allyl π^* and $\phi^b(d_{x^2-z^2})$ orbitals, becomes lower in energy with the decrease in θ (see Chart 2 for $\psi(\phi^b(d_{x^2-z^2})\text{-}\pi^*)$). This is because the overlap between $\phi^b(d_{x^2-z^2})$ and the p_π orbital of the π-allyl C_c atom is enhanced with the decrease in θ. At the same time, $\psi(n\pi\text{-}\phi^a(d_{x^2-z^2}))$, which is mainly composed of the bonding interaction between the π-allyl nπ and $\phi^a(d_{x^2-z^2})$ orbitals, becomes lower in energy with the decrease in θ and reaches the minimum around $\theta = 90°$. This is because the maximum overlap between the π-allyl nπ and $\phi^a(d_{x^2-z^2})$ orbitals occurs at $\theta = 90°$ (note that the nπ orbital expands perpendicularly to the π-allyl plane). It should be also noted that $\psi(\phi^b(d_{xz})\text{-}\pi)$ slightly increases in energy with the decrease in θ. This orbital mainly consists of an antibonding interaction between π-allyl π and $\phi^b(d_{xz})$ orbitals, into which the π-allyl π^* orbital mixes in a bonding way with $\phi^b(d_{xz})$, as shown in Figure 2. In Chart 2, we expected that the back-donating interaction between $\phi^b(d_{xz})$ and π-allyl π^* orbitals is enhanced with the decrease in θ. This expectation seems to be inconsistent with the energy change of $\psi(\phi^b(d_{xz})\text{-}\pi)$ observed in Figure 2. This apparent inconsistency will be discussed below in more detail.

(24) (a) Reed, A. E.; Weinstock, R. B.; Weinhold, F. *J. Chem. Phys.* **1985**, *83*, 735. (b) Reed, A. E.; Curtiss, L. A.; Weinhold, F. *Chem. Rev.* **1988**, *88*, 899.

Chart 2

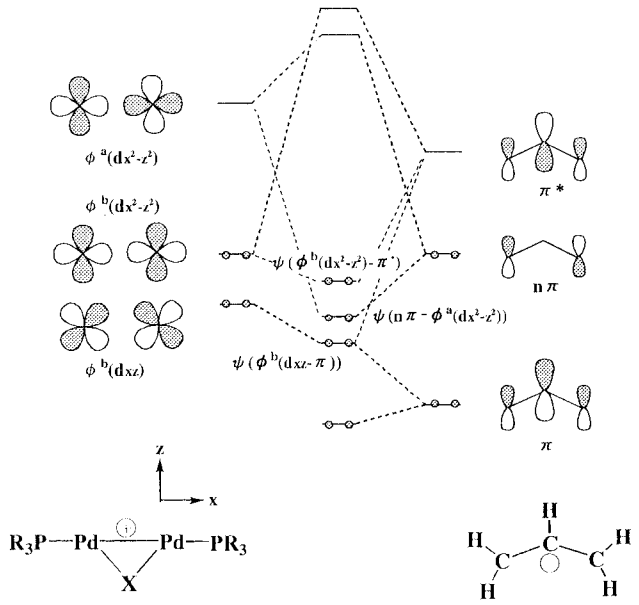

(A) Orbital interaction diagram of $Pd_2(\mu\text{-}X)(\mu\text{-}C_3H_5)(PH_3)_2$

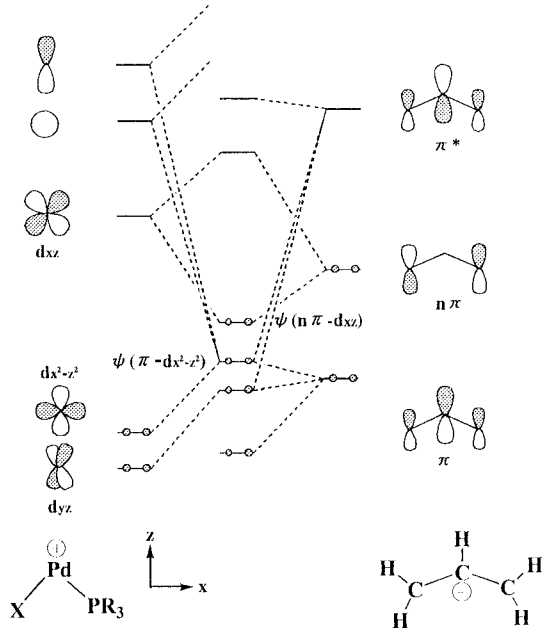

(B) Orbital interaction diagram of $PdX(\eta^3\text{-}C_3H_5)(PH_3)$

Chart 3

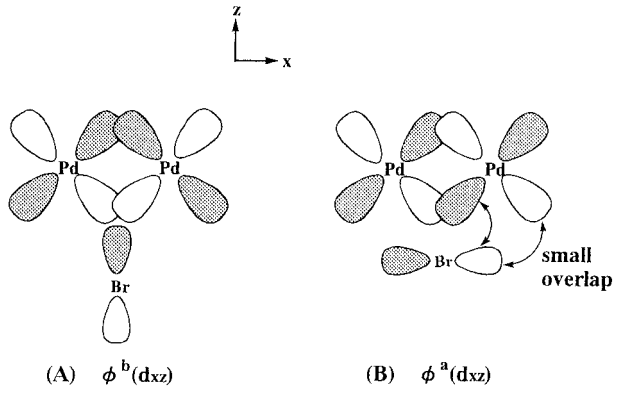

Chart 4

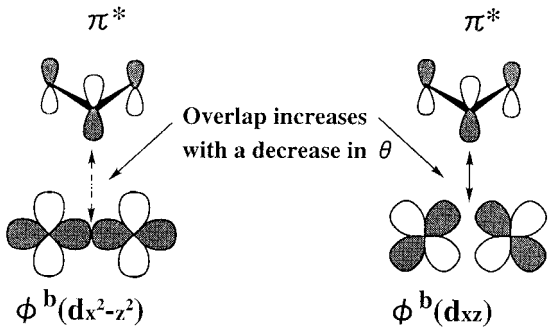

For mononuclear Pd(II) π-allyl complexes, a Walsh diagram is examined in $[Pd(\eta^3\text{-}C_3H_5)(PH_3)_2]^+$ (**3**) instead of **2**, since the higher symmetry of **3** than that of **2** allows us to analyze easily the bonding nature. The dihedral angle of **3** was calculated to be 114° (see Table 2), being a little bit smaller than the experimental value of $[Pd(\eta^3\text{-}C_3H_4\text{-}CH_3)(PMe_3)_2]^+$.[21] However, the dihedral angle of cationic palladium(II) π-allyl complexes seems sensitive to the coexisting ligand and is reported to be in the range of 104−120°.[25] The optimized dihedral angle is in the reported range. Moreover, the optimized angle is much larger than 90°. Thus, **3** is expected to provide a clear reason that the dihedral angle is larger than 90° in the mononuclear palladium(II) π-allyl complexes.

As apparently shown in Figure 3, $\psi(n\pi\text{-}d_{xz})$ and $\psi(\pi\text{-}d_{x^2-z^2})$ become lower in energy with the increase in θ. $\psi(\pi\text{-}d_{x^2-z^2})$ involves the antibonding overlap between π-allyl π and Pd $d_{x^2-z^2}$ orbitals, which decreases with the increase in θ, as shown in Chart 5A. Thus, $\psi(\pi\text{-}d_{x^2-z^2})$ becomes lower in energy as θ increases. Because $\psi(n\pi\text{-}d_{xz})$ involves the bonding overlap between Pd d_{xz} and π-allyl nπ orbitals, the above-mentioned energy change in $\psi(n\pi\text{-}d_{xz})$ indicates that the donating interaction strengthens with the increase in θ. If we forget the detailed consideration of the geometry, this seems unreasonable, as follows: since the π-allyl nπ orbital expands perpendicularly to the π-allyl plane, the overlap between the nπ and d_{xz} orbitals is the greatest at θ = 90°. This is certainly true if the C_t atoms of π-allyl lie on the $Pd(PH_3)_2$ plane. However, the C_t atoms take their positions under the $Pd(PH_3)_2$ plane. Thus, the increase in θ enhances the bonding overlap between the π-allyl nπ and Pd d_{xz} orbitals, as shown in Chart 5B.

The next question is why the C_t atoms of π-allyl take their positions under the $Pd(PH_3)_2$ plane in **3**. This

(25) (a) The dihedral angle is 104° for $[Pd(\eta^3\text{-}CH_2CCHCH_2\text{-}CH_2CH_2)(biquinoline)](CF_3SO_3)$,[25b] 107.4° for $[Pd(\eta^3\text{-}2\text{-}MeC_3H_4)\{R^1N{=}C(PdCl_2L)CMe{=}NR^2\}]$ (L = PPh_3; $R^1 = R^2 = C_6H_4OMe\text{-}P$),[25c] 108° for $Pd[(\eta^3\text{-}R_1R_2CCHCH_2)(N{-}N)](PF_6)$ ($R_1R_2 = (CH_2)_3$; N−N = bidentate diamine),[25d] 109.4° for $[Pd(\eta^3\text{-}C_4H_7)(bpy)](CF_3SO_3)$ (bpy = 2,2′-bipyridine),[25e] and 113.9° for $[Pd(\eta^3\text{-}2\text{-}MeC_3H_4)(dps)][Pd(\eta^3\text{-}2\text{-}MeC_3H_4)Cl_2]$ (dps = di-2-pyridyl sulfide).[25f] (b) Albinati, A.; Ammann, C.; Pregosin, P. S.; Rüegger, H. *Organometallics* **1990**, *9*, 1826. (c) Crociani, B.; Bertani, R.; Boschi, T.; Bandoli, G. *J. Chem. Soc., Dalton. Trans.* **1982**, 1715. (d) Togni, A.; Rihs, G.; Pregosin, P. S.; Ammann, C. *Helv. Chim. Acta*. **1990**, *73*, 723. (e) Albinati, A.; Kunz, R. W.; Ammann, C. J.; Pregosin, P. S. *Organometallics* **1991**, *10*, 1800. (f) Munno, G. D.; Bruno, G.; Rotondo, E.; Giordano, G.; Schiavo, S. L.; Piraino, R.; Tresoldi, G. *Inorg. Chim. Acta*. **1993**, *208*, 67.

Table 3. Electron Distribution[a] of $M_2(\mu\text{-}X)(\mu\text{-}C_3H_4R)(PH_3)_2$, (M = Pd or Pt; X = Cl or Br; R = H, CH_3, or CN), $PdCl(\eta^3\text{-}C_3H_4R)(PH_3)$, and $[Pd(\eta^3\text{-}C_3H_5)(PH_3)_2]^+$

	M = Pd				M = Pt				
	X = Cl	X = Br			X = Br	$PdCl(\eta^3\text{-}C_3H_4R)(PH_3)$			
	R = H	R = H	R = CH_3	R = CN	R = H	R = H	R = CH_3	R = CN	$[Pd(\eta^3\text{-}C_3H_5)(PH_3)_2]^+$
Pd	0.252	0.300	0.281	0.245	0.123	0.360	0.363	0.388	0.307
C_3H_4R	−0.235	−0.252	−0.241	−0.345	−0.298	0.048	0.049	−0.027	0.192

[a] NBO analysis by the MP2/BS-II calculation. [b] C_{t1} (see Chart 1). [c] C_{t2} (see Chart 1).

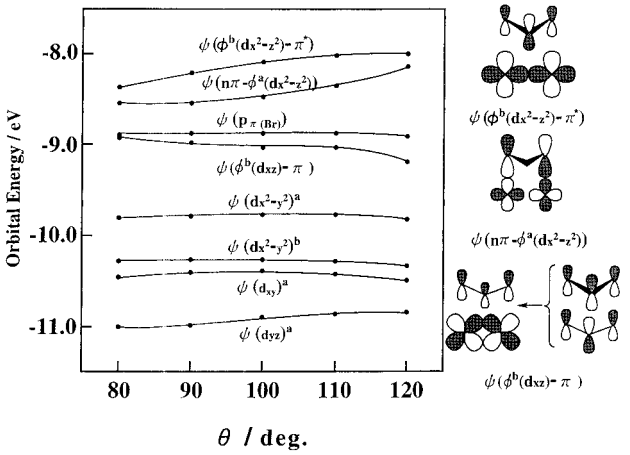

Figure 2. Occupied orbital energies vs dihedral angle (θ) in $Pd_2(\mu\text{-Br})(\mu\text{-}C_3H_5)(PH_3)_2$. See Chart 2 and right-hand side of this figure for $\psi(\phi^b(d_{x^2-z^2})\text{-}\pi^*)$, etc.[23] The superscripts of a and b represent an antibonding overlap between two $d_{x^2-z^2}$ orbitals and a bonding overlap between them, respectively.

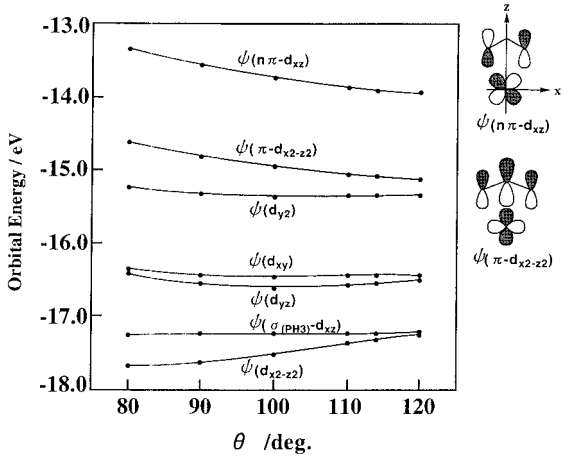

Figure 3. Occupied orbital energies vs dihedral angle (θ) in $[Pd(\eta^3\text{-}C_3H_5)(PH_3)_2]^+$. (a) The C_t atoms are placed at the optimized position of $[Pd(\eta^3\text{-}C_3H_5)(PH_3)_2]^+$.

geometrical feature of mononuclear palladium(II) π-allyl complexes has been well known for a long time,[9] but a conclusive discussion has not been presented yet to our knowledge. We examined the dihedral angle when two C_t atoms exist on the $Pd(PH_3)_2$ plane. Although the dihedral angle of 90° is the most favorable for the donating interaction with the π-allyl nπ orbital, the energy minimum appears around θ = 110°, as shown in Figure 4. $\psi(\pi\text{-}d_{x^2-z^2})$ becomes lower in energy with the increase in θ, which is responsible for the increase in θ. The other orbitals do not participate in the increase of θ. As described above, the π-allyl π orbital suffers from the antibonding mixing of the $d_{x^2-z^2}$ orbital. Thus, the dihedral angle θ increases to 110° to weaken the $d_{x^2-z^2}$ antibonding mixing.

Chart 5

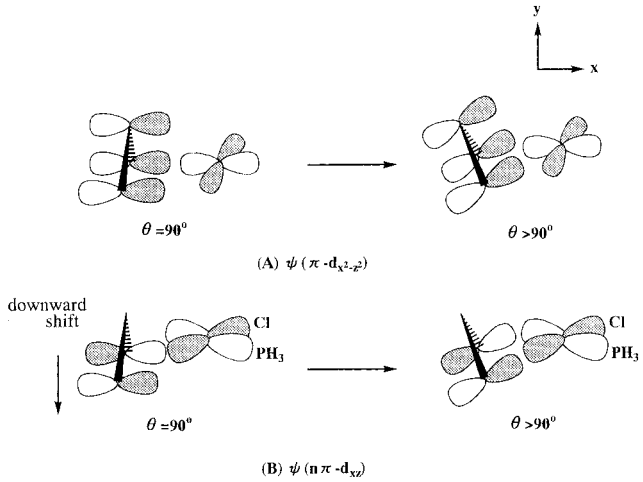

From the above discussion, a coherent picture might emerge as follows: In mononuclear palladium(II) π-allyl complexes, the dihedral angle increases to weaken the antibonding mixing between the π-allyl π and Pd $d_{x^2-z^2}$ orbitals. This leads to a decrease in the bonding overlap between π-allyl nπ and Pd d_{xz} orbitals if the C_t atoms exist on the $Pd(PH_3)_2$ plane. However, the increase in the dihedral angle enlarges the n$\pi-d_{xz}$ bonding overlap (see Chart 5B) when the downward shift occurs. In other words, the downward shift necessarily occurs to weaken the $\pi-d_{x^2-z^2}$ antibonding mixing with little weakening of the n$\pi-d_{xz}$ bonding overlap.

Here, we should notice the difference between $\psi(\pi\text{-}d_{x^2-z^2})$ of **3** and $\psi(\phi^b(d_{xz})\text{-}\pi)$ of **1Br-H**: as θ decreases, the former increases in energy to a greater extent than the latter.[26] This difference between **1Br-H** and **3** is easily understood in terms of the back-donating interaction. In **3**, the π-allyl π^* orbital might mix into $\psi(\pi\text{-}d_{x^2-z^2})$ because they are in the a_1 representation of the C_s symmetry. However, the back-donating interaction is weak, as clearly shown by the positive population of the π-allyl part (see above and Table 3), because the Pd d orbitals lie at low energies due to the 2+ oxidation state of Pd. This means that the π-allyl π^* orbital mixes little in a bonding way with the Pd $d_{x^2-z^2}$ orbital.[27] As a result, the decrease in θ enhances only the antibonding overlap between Pd $d_{x^2-z^2}$ and π-allyl π orbitals, which leads to the considerable energy destabilization of $\psi(\pi\text{-}d_{x^2-z^2})$ with the decrease in θ. In **1Br-H**, on the other hand, the back-donating interaction between Pd d_{xz} and π-allyl π^* orbitals considerably participates in

(26) When θ decreases from 120° to 80°, $\psi(\phi^b(d_{xz})\text{-}\pi)$ increases in energy by 0.25 eV in **1Br-H**, but $\psi(\pi\text{-}d_{x^2-z^2})$ increases by 0.50 eV in **3**.

(27) The Pd d_{yz} orbital would participate more in the back-donating interaction with the π-allyl π^* orbital than the $d_{x^2-z^2}$ orbital. Since Pd d_{yz} and $d_{x^2-z^2}$ orbitals are in the same a_1 representation of the C_s symmetry, the d_{yz} orbital might mix into $\phi(\pi\text{-}d_{x^2-z^2})$ and lower $\phi(\pi\text{-}d_{x^2-y^2})$ in energy if the back-donating interaction is strong.

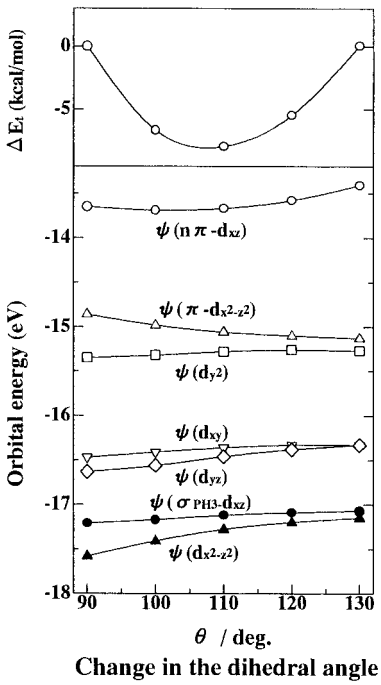

Figure 4. Total energy and orbital energies vs the dihedral angle (θ) of π-allyl in $[Pd(\eta^3\text{-}C_3H_5)(PH_3)_2]^+$. The structure with the dihedral angle of 90° is taken to be a standard (energy zero). The C_t atoms lie on the $Pd(PH_3)_2$ plane.

the bonding interaction between Pd and π-allyl, as clearly shown by the negative charge on the μ-C_3H_5 part (Table 3). Thus, the small θ angle leads to the large overlap between the π-allyl C_c p_π orbital and $\phi^b(d_{xz})$ (see Chart 4), which enhances the antibonding overlap between $\phi^b(d_{xz})$ and π-allyl π orbitals and, at the same time, the back-donating interaction between $\phi^b(d_{xz})$ and π-allyl π^* orbitals. The increase in the antibonding overlap is mostly compensated by the increase in the back-donating interaction. Thus, $\psi(\phi^b(d_{xz})\text{-}\pi)$ of **1Br-H** increases in energy to a much lesser extent than $\psi(\pi\text{-}d_{x^2-z^2})$ of **3** as θ decreases,[26] which does not favor the large θ angle of **1Br-H**, unlike that of **3**.

In summary, the back-donating interaction from Pd(I) to π-allyl is strong in **1**, which leads to the small dihedral angle of about 85° between π-allyl and $Pd_2(\mu\text{-}X)$ planes. On the other hand, only the donating interaction from π-allyl to Pd(II) contributes to the π-allyl coordinate bond in **3**. As a result, the dihedral angle θ is greater than 90° in mononuclear Pd(II) π-allyl complexes.

Substituent Effects on the Dihedral Angle and the C_t−C_c Bond Distance. Since the dihedral angle θ of **1** depends on the back-donating interaction, introduction of an electron-withdrawing group is expected to decrease the dihedral angle. Thus, we investigate the substituent effects on the dihedral angle in **1** and **2**, where the substituent is introduced on the C_c atom because the substituent on the C_c atom would more influence the π-allyl π^* orbital than that on the C_t atom (note that the p_π orbital of the C_c atom contributes more to the π^* orbital than that of the C_t atom). As shown in Table 4, $Pd_2(\mu\text{-Br})(\mu\text{-}C_3H_4\text{-}CH_3)(PH_3)_2$ (**1Br-Me**) has almost the same θ value as that of **1Br-H**. C_3H_4-Me has the π and π^* orbitals at a higher energy than those of C_3H_5 (Figure 5),[28] probably because of the electron-releasing effect of CH_3, while its $n\pi$ orbital lies at almost the same energy as that of C_3H_5. Consistent with their orbital energies, the C_3H_4-Me group of **1Br-Me** is the least negatively charged in **1Br-R** (Table 3). These results clearly indicate that the back-donating interaction of **1Br-Me** is the weakest in **1Br-R**. Nevertheless, the dihedral angle θ is calculated to be almost the same as that in **1Br-H**. This means that the dihedral angle is not very sensitive to the back-donating interaction.

On the other hand, $Pd_2(\mu\text{-Br})(\mu\text{-}C_3H_4CN)(PH_3)_2$ (**1Br-CN**) has a significantly small θ angle of 81°. This small θ value can be explained in terms of frontier orbital energies of C_3H_4CN. As shown in Figure 5, the π^* orbital of C_3H_4CN lies at a considerably lower energy than those of C_3H_5 and C_3H_4-Me, which significantly enhances the back-donating interaction from $Pd_2(\mu\text{-Br})(PH_3)_2$ to μ-C_3H_4CN. This strong back-donation is reflected in the largest electron population of C_3H_4CN, as given in Table 3. Although the dihedral angle is not very sensitive to the back-donating interaction of **1Br-Me**, the π^* orbital of C_3H_4-CN lies at a very low energy; therefore, the back-donation is significantly strong, which decreases the dihedral angle in **1Br-CN**.

Table 4. Important Optimized Geometries[a] of $Pd_2(\mu\text{-Br})(\mu\text{-}C_3H_4R)(PH_3)_2$ (1Br), $Pt_2(\mu\text{-Br})(\mu\text{-}C_3H_5)(PH_3)_2$ (1Pt), and $PdCl(\eta^3\text{-}C_3H_4R)(PH_3)$ (2)

	1Br		1Pt		2	
	R = CH_3	R = CN	R = H		R = CH_3	R = CN
M−M	2.629	2.636	2.650	M-C_{t1}	2.171	2.175
M−C_t	2.116	2.105	2.077	M-C_{t2}	2.141	2.140
M−C_c	2.533	2.483	2.434	M-C_c	2.141	2.128
				C_c−C_{t1}	1.418	1.419
C_t−C_c	1.430	1.436	1.449	C_c-C_{t2}	1.421	1.424
θ	84	81	76	θ	111	127

[a] MP2 optimization with BS-I including polarization functions.

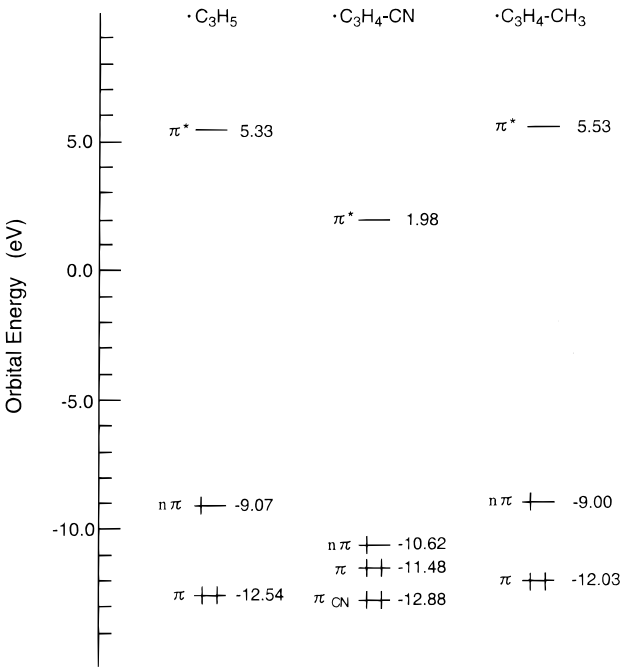

Figure 5. Energy levels of frontier orbitals of the allyl radical.[28]

(28) Because the C_3H_4R group is considered not to be an anion but to be rather neutral in π-allyl complexes, orbital energies were calculated for the C_3H_4R radical.

Table 5. Relative Stabilities, ΔE (kcal/mol),[a] of $Pd_2(\mu\text{-Br})(\mu\text{-CH}_2\text{CRCH}_2)(PH_3)_2$ and $PdCl(\eta^3\text{-CH}_2\text{CRCH}_2)(PH_3)$

R	CH_3	CN
HF	−3.0	6.5
MP2	−2.4	4.3
MP3	−2.5	6.2
MP4DQ	−2.7	5.1
MP4SDQ	−2.8	4.3

[a] $\Delta E = E_t$(right-hand side of eq 1) − E_t(left-hand side of eq 1). A positive value indicates that $Pd_2(\mu\text{-Br})(\mu\text{-CH}_2\text{CRCH}_2)(PH_3)_2$ is more stable than $PdCl(\eta^3\text{-CH}_2\text{CRCH}_2)(PH_3)$. BS-II was used.

The back-donation also leads to the C_t-C_c bond lengthening, since electrons are populated on the π-allyl π^* orbital by the back-donation. Certainly, the C_t-C_c bond lengthens by 0.020 Å upon going to **1Br-Me** from the free C_3H_4-Me^- and by 0.034 Å upon going to **1Br-H** from the free $C_3H_5^-$. These results are consistent with the back-donation being stronger in **1Br-H** than in **1Br-Me**. However, the C_t-C_c bond of **1Br-CN** lengthens by only 0.033 Å compared to the free C_3H_4-CN^-, being similar to the bond lengthening of **1Br-H**. This is seemingly against our expectation but is easily understood in terms of the C_3H_4-CN^- π^* orbital. Since the π^* orbital is not localized in the allyl C_3 part but delocalized to the C_c-CN bond, not only does the C_t-C_c bond lengthen but also the C_c-CN bond shortens by 0.012 Å upon coordination of C_3H_4-CN^- (note that the π^* orbital of C_3H_4-CN^- involves a bonding interaction between C_c p_π and CN π^* orbitals). This means that electrons are populated not only on the C_t-C_c part but also on the C_c-CN part, and as a result, the C_t-C_c bond lengthens less than expected. The difference in the C_t-C_c distance between **1** and **2** is also related to the bonding nature. The C_t-C_c distance of **1** is slightly longer than that of **2** by 0.01 Å, except for **1Br-Me**, in which the back-donation is weak (see Tables 1, 2, and 4). This is consistent with the stronger back-donation in **1** than in **2**.

Substituent Effects on the Relative Stabilities of Dinuclear Palladium(I) μ-Allyl and Mononuclear Palladium(II) π-Allyl Complexes. The equilibrium constant K of eq 1 significantly depends on the substituent introduced on π-allyl.[8b] This dependence

$$Pd_2(\mu\text{-Br})(\mu\text{-}C_3H_4R)(PH_3)_2 + PdCl(\eta^3\text{-}C_3H_5)(PH_3) \rightleftarrows Pd_2(\mu\text{-Br})(\mu\text{-}C_3H_5)(PH_3)_2 + PdCl(\eta^3\text{-}C_3H_4R)(PH_3) \quad (1)$$

should be related to the bonding nature of **1** and **2**. Here, we wish to estimate theoretically the relative stabilities of **1** and **2** and then to explain them on the basis of bonding nature. The energy difference between the right- and left-hand sides of eq 1 is given in Table 5, where the positive value represents that the left-hand side is more stable than the right-hand side. Apparently, the CH_3 group favors the right-hand side of eq 1. In other words, the CH_3-substituted π-allyl group prefers the mononuclear palladium(II) complex to the dinuclear palladium(I) complex. On the other hand, the CN-substituted π-allyl group favors the left-hand side. This means that the electron-withdrawing group stabilizes the dinuclear palladium(I) complex.

As shown above, **1Br-CN** involves the strongest back-donating interaction. This strongest back-donating interaction yields both the smallest dihedral angle and the largest energy destabilization of eq 1. **1Br-Me** involves the least back-donating interaction, as discussed above. This would be a main reason that C_3H_4-Me prefers the mononuclear palladium(II) complex to the dinuclear palladium(I) complex. The equilibrium constant of eq 1 seems to be more sensitive to the bonding nature and a better measure of back-donating interaction than the dihedral angle.

A Comparison between Pt and Pd. Although a platinum(I) dinuclear μ-allyl complex, $Pt_2(\mu\text{-X})(\mu\text{-}C_3H_5)(PR_3)_2$, has not been known experimentally, its comparison with the Pd analogue would be interesting. We optimized here $Pt_2(\mu\text{-Br})(\mu\text{-}C_3H_5)(PH_3)_2$ (**1Pt**) with the MP2/BS-I method. As shown in Table 4, there are several interesting differences between Pt and Pd: (1) the Pt−Pt distance of **1Pt** is slightly longer than Pd−Pd of **1Br-H**; (2) the C_t-C_c distance of **1Pt** is longer than that of **1Br-H**; (3) the $C_tC_cC_t$ angle of **1Pt** is larger than that of **1Br-H**; and (4) the dihedral angle θ of **1Pt** is considerably smaller than that of **1Br-H**. Although the dihedral angle of $PtPd(\mu\text{-Br})\{\mu\text{-}CH_2C(CO_2Me)CH_2\}(PPh_3)_2$ was reported to be almost the same as that of the Pd analogue,[8b] the small dihedral angle of **1Pt** optimized here seems reasonable, as follows: In general, the Pt d orbital is at a higher energy than the Pd d orbital. Actually, $\phi^a(d_{x^2-z^2})$ and $\phi^b(d_{x^2-z^2})$ of $[Pt_2(\mu\text{-Br})(PH_3)_2]^+$ are calculated to be at higher energies than those of $[Pd_2(\mu\text{-Br})(PH_3)_2]^+$; $\phi^a(d_{x^2-z^2})$ is −5.57 eV in the Pd system and −4.99 eV in the Pt system, and $\phi^b(d_{x^2-z^2})$ is −12.95 eV in the Pd system and −12.71 eV in the Pt system. Thus, the donating interaction becomes weak but the back-donating interaction becomes strong in **1Pt**, which would decrease the dihedral angle. The strong back-donating interaction certainly is reflected in the electron distribution, as shown in Table 2; the C_3H_5 group in **1Pt** is more negatively charged than that in **1Br-H**. Also, the long C_t-C_c bond of **1Pt** arises from the strong back-donating interaction. Thus, it is worthwhile to synthesize the platinum(I) dinuclear μ-allyl complex, to investigate its electron distribution, bonding nature, and relative stabilities, and to compare them with those of the dinuclear palladium(I) μ-allyl complex.

Concluding Remarks

A series of dinuclear palladium(I) μ-allyl complexes, $Pd_2(\mu\text{-X})(\mu\text{-}C_3H_4\text{-R})(PH_3)_2$ (**1**), and mononuclear palladium(II) π-allyl complexes, $PdCl(\eta^3\text{-}C_3H_4\text{-R})(PH_3)$ (**2**) and $[Pd(\eta^3\text{-}C_3H_5)(PH_3)_2]^+$ (**3**), are theoretically investigated in detail with the ab initio MO method. In **1**, the μ-allyl coordinate bond is formed through the donating interaction between the π-allyl nπ orbital and the Pd−Pd $d_{x^2-z^2}$ antibonding MO and the back-donating interaction between the π-allyl π^* orbital and the Pd−Pd $d_{x^2-z^2}$ bonding MO. The palladium atoms take their positions under the terminal carbon atoms of μ-allyl to maximize these two interactions. The dihedral angle θ between μ-allyl and $Pd_2(\mu\text{-X})$ planes decreases to about 85° from 90° to strengthen the above-mentioned back-donating interaction and the other back-donating interaction between π-allyl π^* and Pd−Pd d_{xz} bonding orbitals. In **2** and **3**, on the other hand, only the donating interaction between η^3-allyl nπ and the palladium(II) unoccupied d orbital contributes to the η^3-allyl coordinate bond. The dihedral angle θ increases to strengthen the donating interaction and to weaken

the antibonding overlap between the η^3-allyl π and Pd $d_{x^2-z^2}$ orbitals. A Walsh diagram provides strong support for the above explanation.

Introduction of a CN group to π-allyl decreases the dihedral angle in **1**, because the CN group strengthens the back-donating interaction in **1**, as expected. Because of this strong back-donating interaction, the CN-introduced π-allyl group prefers $Pd_2(\mu\text{-Br})(\mu\text{-}C_3H_4\text{-CN})(PH_3)_2$ to $PdCl(\eta^3\text{-}C_3H_4\text{-CN})(PH_3)$. On the other hand, introduction of a CH_3 group destabilizes $Pd_2(\mu\text{-Br})(\mu\text{-}C_3H_4\text{-Me})(PH_3)_2$ relative to $PdCl(\eta^3\text{-}C_3H_4\text{-Me})(PH_3)$, because the CH_3 group weakens the back-donating interaction. However, the dihedral angle θ of $Pd_2(\mu\text{-Br})(\mu\text{-}C_3H_4\text{-Me})(PH_3)_2$ changes little upon introduction of the CH_3 group. Thus, the equilibrium constant K of eq 1 is a better measure for the donation and back-donation interactions than the dihedral angle.

Acknowledgment. The authors thank the Ministry of Education, Science, Sports, and Culture for financial support by Grants-in-Aid for Scientific Research on Priority Area.

Supporting Information Available: Tables of optimized geometrical parameters for **1**, **2**, and **3** (3 pages). Ordering information is given on any current masthead page.

OM970115K